Effect of slope geometry on stability of slope in Almaty

Alfrendo Satyanaga[1*], *Rezat* Abishev[2], *Assylanbek* Sharipov[2], *Martin* Wijaya[3], *Abdul Halim* Hamdany[4], *Sung-Woo* Moon[1], and *Jong* Kim[5]

[1]Assistant professor, Department of Civil and Environmental Engineering, Nazarbayev University, 53 Kabanbay Batyr, Kazakhstan
[2]Research Scholar, Department of Civil and Environmental Engineering, Nazarbayev University, 53 Kabanbay Batyr, Kazakhstan
[3]Professor, Department of Civil and Environmental Engineering, Nazarbayev University, 53 Kabanbay Batyr, Kazakhstan
[4]Lecturer, Faculty of engineering, Civil Engineering Department, Universitas Katolik Parahyangan, Bandung, Jawa Barat, Indonesia
[5]Lecturer, Department of Civil Engineering, University of Indonesia, Indonesia

Abstract. Landslides bring destruction to buildings, and nearby located structures and mostly occur in rural areas. Such hazard commonly takes place in mountainous areas in Central Asia. Kazakhstan region has highly vulnerable areas to rainfall-induced landslides in South-Eastern parts due to presence of many mountains. The purpose of the research is to demonstrate the effect of slope geometry on slope stability under heavy rainfall in Almaty, Kazakhstan. Transient seepage analyses were conducted using Seep/W while limit equilibrium slope stability analyses were performed using Slope/W. 15 sets of numerical analyses were carried out on different slope angle and slope height incorporating the soil-water characteristic curve and unsaturated permeability and unsaturated shear strength of soil from Almaty. According to the obtained simulation results in GeoStudio software for seepage analysis, the pore-water pressure is increased almost for 80 kPa at the mid slope of each simulation. The change of FoS for the gentlest slope with 27 degrees slope angle is the lowest for 10 m slope height and the highest for 30 m slope height, whereas the change of FoS for slope with 45 degrees of slope angle (9%) is almost the same for all slope height.

1 Introduction

Beginning from past decades up to recent days, one of the major concerns worldwide is considered to be a tendency of global warming and climate change. By definition, climate change is abiding variations in temperature and weather patterns [1]. However, the temperature since the 19th century is continuously rising due to the routine of burning fossil fuels like gas, coal, and oil by humanity. The main effects of temperature change are affected weather conditions [2]. For instance, an increase in drought seasons, and the shrinking of ice sheets result in the growth of sea levels and the intensity of rainfall patterns [3, 4].

In terms of rainfall precipitation, the paper focuses on the Kazakhstan region located in Central Asia. According to Jiang et al. (2020), the annual mean rainfall in the Central Asia region demonstrates a moderate rise from 1920 to 2010 [5]. However, the precipitation tends to increase rapidly from 2010 to 2100, based on simulation model results. Hence, the increase in rainfall intensilty may lead to several hazards, namely floods, droughts, and landslides [6].

Kazakhstan region has highly vulnerable areas to rainfall-induced landslides in the South-Eastern parts due to mountains [6]. Additionally, the soil movement on slopes may harm the surroundings and residents of Almaty city, which is located in the aforementioned region [7]. Landslides lead to destruction of buildings and nearby located structures. Such hazard commonly takes place in mountainous areas in Central Asia. One of the main causes is regarded to be a hydrological anomaly in terms of intensive rainfalls [7, 8]. Moreover, the author highlights Almaty city is exposed to rainfall-induced landslides. Chepelianskaia and Sarkar-Swaisgood (2022) indicated that South-Eastern Kazakhstan is highly exposed to landslide risks, where Almaty city is located [6]. At the moment, there is limited study on the effect of rainfall triggering landslides incorporating unsaturated soil mechanics principles in Kazakhstan. In addition, there is no study investigating the effect of slope geometry on the stability of slopes in Kazakhstan.

The research aims to demonstrate slope geometry's influence on slope stability under heavy rainfall in Kazakhstan via numerical analysis. Seepage analyses, including soil-water characteristic curve (SWCC) and permeability function, were conducted to demonstrate pore-water pressure changes against depth with time. The stability analyses were performed to demonstrate slope stability in terms of the factor of safety versus time during precipitation and dry periods.

2 The investigated soils

The appropriate soil is taken from the research of Satyanaga et al. (2022) [9]. The selected soil is clayey soil from Almaty. Properties of the investigated soil from the Almaty region are presented in Table 1.

1* Corresponding author: alfrendo.satyanaga@nu.edu.kz

Table 1. Soil engineering properties [10].

Characteristic	Clayey loam
Total density ρ, g/cm³	*1.73*
Dry density ρ_d, g/cm³	*1.45*
Specific gravity ρ_s, g/cm³	*2.7*
Moisture content W	*0.188*
Void ratio e	*0.861*
Effective cohesion c', kPa	*33*
Effective friction angle ϕ', deg	*19*
Unsaturated shear strength ϕ^b, deg	*12.7*
Compression modulus E, MPa	*7.4*

The water table is located at a depth of 3 meters to a minimum of 10 meters for Almaty city [11]. The appropriate parameters of clayey loam for estimating of soil hydraulic properties namely SWCC and permeability function were taken according to the study of Satyanaga et al. (2022) and Mercer et al. (2019) [9, 12]. The following equation proposed by Fredlund and Xing (1994) was used to generate continuous curve of SWCC [13]. The permeability function was developed using the implementation of the statistical method [14]. Figures 1 and 2 present the SWCC and permeability function of the investigated soil.

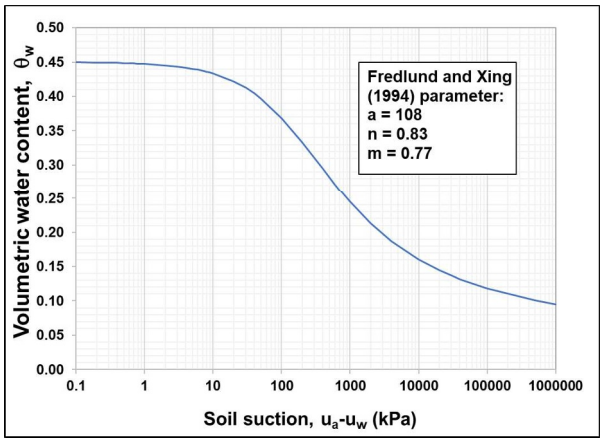

Fig. 1. SWCC curve.

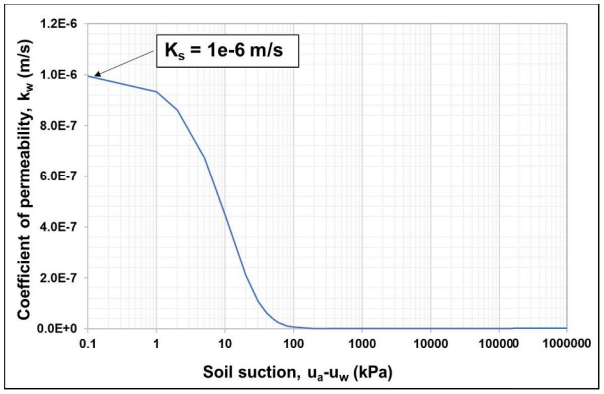

Fig. 2. Permeability function.

3 Research methodology

Seepage analysis was conducted using GeoStudio software, where SEEP/W was utilized to obtain pore-water pressure variations according to the depth of the soil at different slope angles and heights. The transient SEEP/W analysis was selected, and the water table served for initial pore-water pressure and head conditions. The initial rate changed from 1 to 0.65 to improve the convergence rate in the iteration calculation [16].

The unsteady seepage equation is incorporated into SEEP/W analyses [15]. Next, the slope model with corresponding coordinates is constructed. There should be noted that the length of the top and bottom sides of the slope is 3 times the height of the slope. It is an appropriate value to avoid the effect of boundary conditions from the left side and right sides of the numerical model since raindrops may infiltrate to nearby soil on both sides [16]. Different angles and heights of slopes were used for further comparison.

The boundary conditions as the head location for the left and right sides of the slope are incorporated into the model including total, elevation, and pressure head. Chepelianskaia and Sarkar-Swaisgood (2022) emphasize that daily heavy rainfall precipitation in Kazakhstan is about 20 mm [6]. Hence, 20 mm per day is taken as an input value of rainfall and placed on the surface of the built model. An example of the model is illustrated in Figure 3.

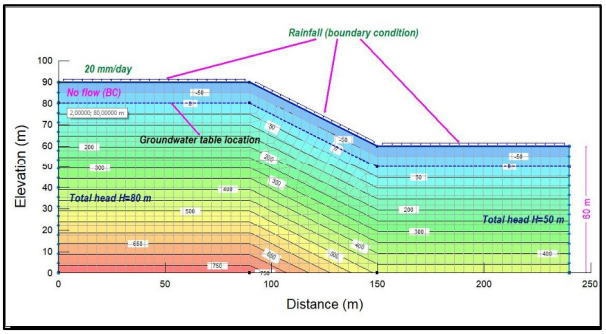

Fig. 3. Slope model in GeoStudio.

The last step is to obtain the contour of pore-water pressure variations in underlying soil during rainfall infiltration. In addition, the graph of pore-water pressure versus depth is illustrated to demonstrate changes at any selected time.

Slope stability analysis is performed based on SEEP/W analysis inputs. Pore-water pressure from SEEP/W is exported to SLOPE/W analysis inputs. The main geotechnical parameters are taken from the study of Khomyakov et al. (2013) for the Almaty region: friction angle, cohesion, and unit weight of clayey loam [10].

SLOPE/W analysis uses two equations of limit equilibrium with respect to moment and force. Slip surface location using grid and radius is a built-in model to analyze the factor of safety versus time for 12 days of continuous rainfall [17]. The graph demonstrates the

change in the factor of safety of soil under the slope due to water infiltration in a time-lapse.

4 Seepage and stability analyses

The simulation is conducted in GeoStudio Software for seepage and slope stability analysis. Three different slope heights of 10, 20, and 30 meters were selected, whereas 27, 35, 45, 60, and 80 slope angles were chosen for the simulation process (Table 2). Figure 3 is the representation of the model for slope with those parameters. The selected angle is 27 degrees and the slope height is 30 meters.

Table 2. Cases with parameters used in GeoStudio.

Case No.	Slope height, m	Slope angle, deg	Precipitation, mm/day	Ground water table depth, m
1	10	27	20	-10
2	10	35	20	-10
3	10	45	20	-10
4	10	60	20	-10
5	10	80	20	-10
6	20	27	20	-10
7	20	35	20	-10
8	20	45	20	-10
9	20	60	20	-10
10	20	80	20	-10
11	30	27	20	-10
12	30	35	20	-10
13	30	45	20	-10
14	30	60	20	-10
15	30	80	20	-10

Seepage analysis represented the pore-water pressure changes during the rainfall. The results from finite element analyses indicated that the pore pressure of soil is increased, and matric suction is decreased. Figure 4 depicts pore-water pressure (PWP) profiles at the beginning of rainfall, on the 4th, 10th, 16th, and 24th days according to the depth beginning from the mid-slope surface. It can be seen that the PWP is extremely low before rainfall starts on the surface. However, it starts to increase to the lower depths due to the location of the ground water table, which is 10 m below the ground surface. On the other hand, the highest PWP is on the 10th day of rainfall, which is almost -20 kPa, but the trend versus depth for 4th, 10th, 16th and 24th day is approximately the same. There should be noted that after 12 days of rainfall, the PWP starts to increase below the ground water table (yellow line in Figure 4). The ground water table was located at 42 m before rainfall started according to Figure 4, while the ground water table location ups to 44 m. It indicates that during the whole period of rainfall precipitation, the amount of water infiltrated into the ground is almost 2 meters with respect to the movement of the ground water table location.

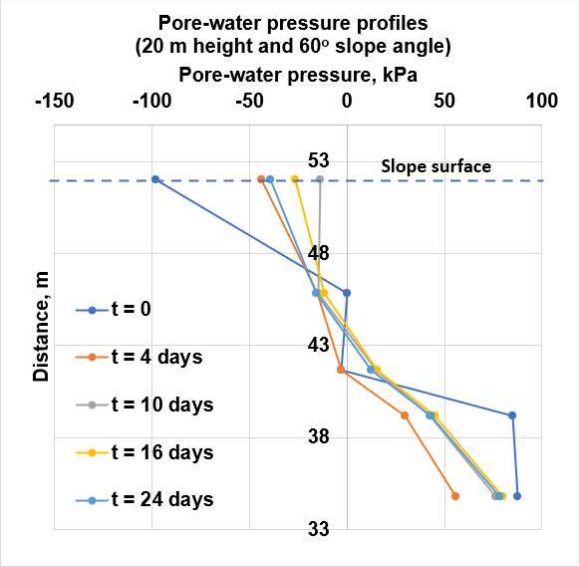

Fig 4. Pore-water pressure profile for 20 m height and 60° angle.

Such a tendency of PWP during the intensive rainfall of 20 mm/day in the Almaty region will cause a sudden reduction of the strength of the underlying slope at any height and slope, which can further be viewed in the reduction of the factor of safety in slope stability analysis. The slope model for stability analysis is developed based on the inputs of SEEP/W analysis. Based on SLOPE/W analysis, the following graph in Figure 5 is developed to demonstrate the factor of safety of soil versus elapsed time in days for the entire period of 24 days. As previously mentioned, rainfall continuously occurs for the first 12 days.

Firstly, it can be observed that the FoS is decreasing for all cases for entire rainfall period, which indicates the loss of shear strength of soil due to raindrop infiltration. Even after 12 days, the FoS is still slightly reduced. It can be explained by the presence of residual water inside the soil that goes through it to deep depths. However, FoS begins to insignificantly increase towards to 24th day from the beginning of the simulation model. It explains the evaporation process and the end of the infiltration process to ground water table and below. The strength also starts to increase.

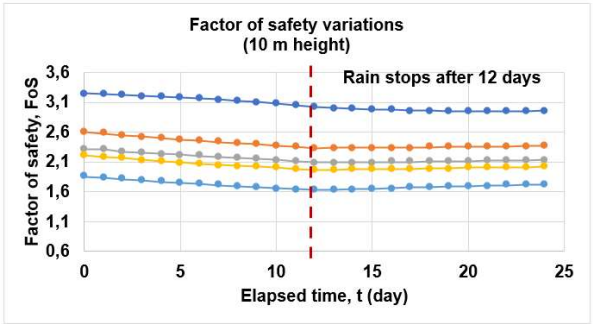

Fig. 5a. 10 m height slope.

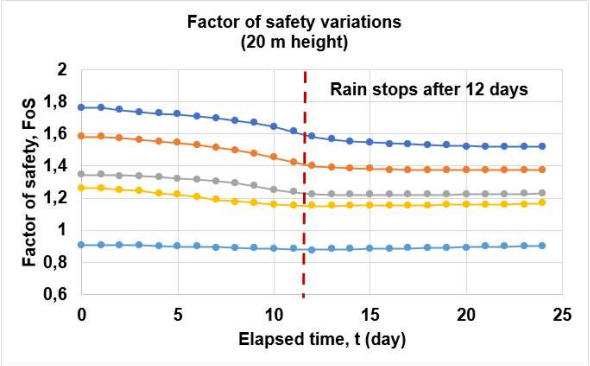

Fig. 5b. 20 m height slope.

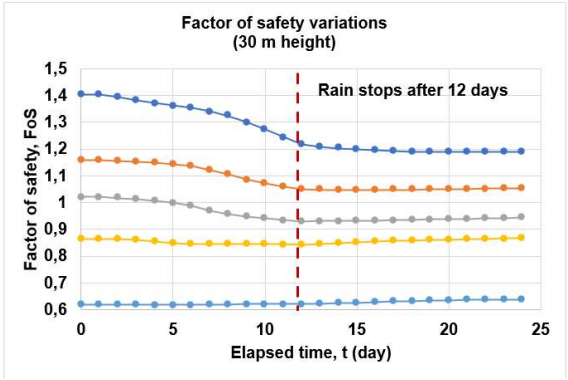

Fig. 5c. 30 m height slope.

Figure 5. A factor of safety variation for different heights with angles (dark blue – 27° angle, orange – 35° angle, green – 45° angle, yellow – 60° angle, light blue – 80°).

5 Discussion

According to Figure 6, the change of FoS for the gentlest slope with 27 degrees slope angle is the lowest for 10 m slope height and the highest for 30 m slope height, whereas the change of FoS for slope with 45 degrees of slope angle (9%) is almost the same for all slope height. On the other hand, Figure 7 represents the reason for the reduction of FoS by implementing pore-water pressure change at the end of rainfall period. PWP is decreased to 82-84% with respect to the initial value for 27 degrees slope, while for 45 degrees, the change decreases to 84-86% for all cases. It can be observed that the change of FoS is reversely proportional to the slope angle for all three cases with respect to steeper slopes. This phenomenon can be explained by the fact that the initial factor of safety is already low for higher slopes, and the change of FoS after rainfall is less than the change of FoS in the shorter slopes. For instance, the change of FoS for slopes with 80 degrees angle and 30 m height slope is approximately 0% at the end of the rainfall period.

There can be observed a tendency of change of FoS from lowest angle to highest for all three cases, where the steeper the angle, change in FoS is lower for higher slopes. For example, 12.29%, 3.34%, -0.32% (Figure 6) for 10 m, 20 m, and 30 m slope heights, respectively. The initial FoS value before the rainfall starts is reversely proportional to slope heights, which indicates that the lowest slopes have high FoS since the steeper slopes are more susceptible to failure or land sliding due to extreme rainfalls. The numerical values of FoS at t=0 (rainfall starts) and t=12 days (rainfall ends) are graphically represented in Figures 8 and 9 for all three cases and five angles. For example, in the case of 27 degrees slope, before rainfall starts, FoS equals to 3.26, 1.76, 1.40 (Figure 11) for slope heights 10, 20, and 30 meters, respectively. For the steepest slope angle (80 degrees), FoS equals 1.86, 0.91, and 0.62 (Figure 11) for 10, 20, and 30 meters, respectively.

Figure 6 also shows almost identical reduction in terms of percentage for all three cases for only 45 degrees steep slope angle. The values are 9.37, 9.07, 8.96% for 10, 20, and 30 m slope heights. It can be named as a breaking point in the observed tendency. There can be concluded that the reduction of FoS is around 9% with respect to the initial value for all slope heights besides three cases at 45 degrees slope.

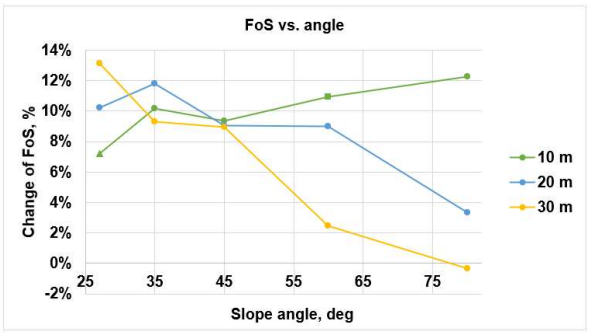

Fig. 6. A factor of safety change at the end of the rainfall against slope angles for three different slope heights.

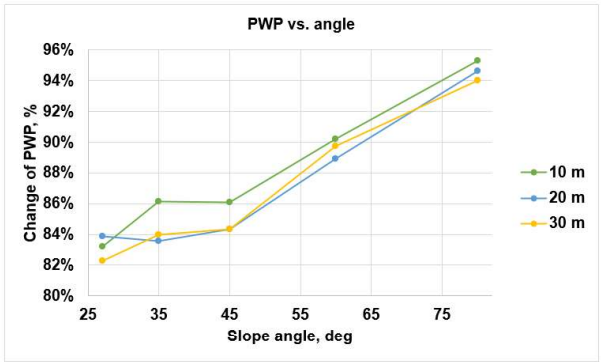

Fig. 7. Pore-water pressure changes at the end of the rainfall against slope angles for three different slope heights.

Overall, some patterns on PWP changes are observed after the rainfall period stops with respect to initial values that obtained before rainfall starts and are graphically represented in Figure 8. A difference indicates the reduction of PWP during the rainfall period, which means the ground water table location is raised due to the infiltration of rain drops into the ground. The change in PWP has the lowest values for the gentlest slope (27 degrees), which are 83, 84, and 82% for 10, 20, and 30 meters, respectively. Reversely, the PWP reduction has the highest amount at the steepest slope (80 degrees). The values are 95, 95, and 94% for 10, 20, and 30 m slope heights, respectively. Therefore, there can be

concluded that the reduction of PWP is proportional to slope angles.

The reason that at steepest slopes the PWP dropped more than in gentle slopes at the midslope surface relates to the flow of runoff and infiltrated raindrops into the ground. When the slope becomes steeper, the flow and drop of rainwater from the top become faster than the gentler slopes. Simultaneously, infiltrated raindrops at the top of the slope flow downward below the slope and affect the sharp change in PWP at the surface of midslope. Figure 7 shows a difference in PWP change between angles 80 and 27 degrees for 12%, 11%, and 11.8% at 10, 20, and 30 m slope height respectively.

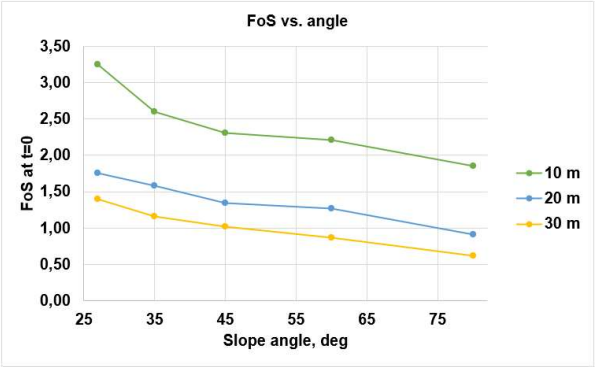

Fig. 8. Factor of safety before the rainfall starts against slope angles for three different slope heights.

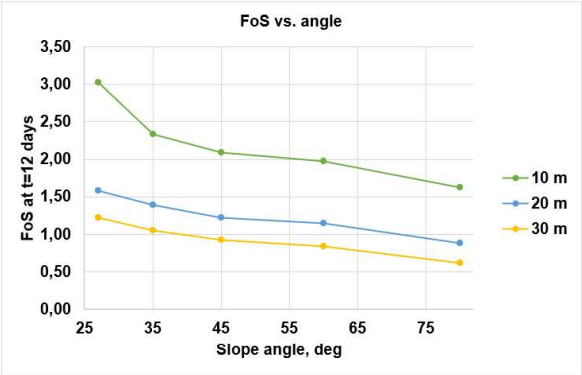

Fig. 9. Factor of safety right after rainfall stops against slope angles for three different slope heights.

6 Conclusions

According to the obtained simulation results in GeoStudio software for seepage analysis, the pore-water pressure is increased to almost 80 kPa at the mid-slope of each simulation. It leads to an increase in suction and a decrease in shear strength of strength. Additionally, slope stability analysis demonstrated that the factor of safety is oppositely proportional to slope height and angle. The change of FoS for the gentlest slope with 27 degrees slope angle is the lowest for 10 m slope height and the highest for 30 m slope height, whereas the change of FoS for slope with 45 degrees of slope angle (9%) is almost the same for all slope height. Nevertheless, the factor of safety tends to reduce for all simulation cases, which confirms the loss of strength of soil due to a large amount of infiltration into the ground. There should be noted that the obtained results are applicable to clayey silt.

Acknowledgements

This research was funded by the Nazarbayev University, Social policy grant and Collaborative Research projects (CRP) Grants No. 11022021CRP1512. Any opinions, findings, conclusions, or recommendations expressed in this material are those of the author(s) and do not necessarily reflect the view of Nazarbayev University.

The authors declare no competing interests.

References

1. N. Gofar, A. Satyanaga, R.Y. Tallar, H. Rahardjo. Geotechnical and Geological Engineering, **40**, 4585-4594 (2022).
2. H. Rahardjo, N. Gofar, A. Satyanaga, E.C. Leong, C.L. Wang, J.L.H. Wong. Journal of Geotechnical and Geological Engineering. (2019a).
3. H. Rahardjo, A. Satyanaga, E.C. Leong, Y.S. Ng, M.D. Foo, C.L. Wang. Proceedings of 10th Australia New Zealand Conference on Geomechanics “Common Ground”. Brisbane, Australia, 21-24 October, Vol.**2**, pp. 704 – 709. (2007)
4. J.R. Kaddo. *Climate Change: Causes, Effects, and Solutions*. A with Honors Projects. April. http://spark.parkland.edu/ah/164. (2016).
5. J. Jiang, T. Zhou, X. Chen, L. Zhang. Environmental Research Letters, April, Vol. **15**. https://doi.org/10.1088/1748-9326/ab7d03. (2020).
6. O. Chepelianskaia, M. Sarkar-Swaisgood. Economic and Social Commission for Asia and the Pacific, March. https://www.unescap.org/kp/2022/5lmaty5tan-climate-change-and-disaster-risk-profile. (2022).
7. M. Thurman. *Natural Disaster Risks in Central Asia: A Synthesis*. Bureau for Crisis Prevention and Recovery – UNDP. https://www.preventionweb.net/publication/natural-disaster-risks-central-asia-synthesis. (2011).
8. C.Y. Ip, H. Rahardjo, A. Satyanaga. Georisk, Assessment and Management of Risk for Engineered Systems and Geohazards, **15:2**, 98-112. (2021).
9. A. Satyanaga, A.B. Ibrahimi, A.S. Mohammad, A.H. Hamdany, M. Wijaya, S.-M. Moon, J. Kim. Water Characteristic Curve for Soils in Kazakhstan.Geotechnical Engineering Journal of the SEAGS & AGSSEA. Accepted in October 2022. (2022).

10. V.A. Khomyakov, E. E. Iskakov and E. T. Serdaliev. Soil Mechanics and Foundation Engineering. September, Vol. **50**, n. 4, pp. 171–177. Doi:10.1007/s11204-013-9230-z. (2013).
11. S. A. King, I. Khalturin Vitaly, B.E. Tucker. Springer Science & Business Media, June. https://books.google.kz/books?id=-u3HBAAAQBAJ&dq=depth+of+groundwater+table+in+6lmaty&source=gbs_navlinks_s. (2013).
12. K. Mercer, H. Rahardjo and A. Satyanaga. Australian Centre for Geomechanics, University of Western Australia. (2019).
13. D. G. Fredlund, A. Xing. Canadian Geotechnical Journal, Vol. **31**, n. 3, pp. 521-532. (1994)
14. H. Rahardjo, A. Satyanaga, H. Mohamed, C. Y. Ip, S. S. Rishi. Journal of Geotechnical and Geological Engineering, April, Vol. **37**, No. 2, pp. 659-672. (2019c).
15. D. G. Fredlund, H. Rahardjo, M. D. Fredlund. "Unsaturated Soil Mechanics in Engineering Practice". John Wiley & Sons, Inc., Hoboken, New Jersey, July. Doi:10.1002/9781118280492; (2012).
16. A. Satyanaga, N. Bairakhmetov, J.R. Kim, S.-W. Moon. *Role of Bimodal Water Retention Curve on The Unsaturated Shear Strength.* Applied Sciences, February, Vol. **12**, n. 1266. Doi: 10.3390/app12031266; (2022a).
17. A. Satyanaga, S.-W. Moon and J.R. Kim. Geomechanics and Engineering, January, Vol. **28**, n. 1, pp. 77-87. Doi: 10.12989/gae.2021.28.1.077; (2022b).
18. A. Satyanaga, H. Rahardjo. Geotechnique. September 2019. Vol. **69**, No. 9, pp. 828-832. (2019).
19. A. Satyanaga, H. Rahardjo. Proceedings of the Institution of Civil Engineers – Geotechnical Engineering, pp. 1–44. Doi:10.1680/jgeen.20.00085; (2020).
20. F. Silva, T. W. Lambe, W. A. Marr. Journal of geotechnical and geoenvironmental engineering, Vol. **134**, n. 12, pp. 1691-1699. https://ascelibrary.org/doi/pdf/10.1061/(ASCE)1090-0241(2008)134%3A12(1691); (2008).
21. H. Rahardjo, A. Satyanaga, E. C. Leong. *Effects of rainfall characteristics on the stability of tropical residual soil slope.* Proceedings of E-UNSAT
22. H. Rahardjo, A. Satyanaga, E.C. Leong, J.-Y. Wang. *Comprehensive Instrumentation for Real Time Monitoring of Flux Boundary Conditions in Slope.* (2014).
23. H. Rahardjo, Y. Kim, A. Satyanaga. International Journal of Geo-Engineering, Vol. **10**, no. 1. Doi:10.1186/s40703-019-0104-8; (2019b).

    H. Rahardjo, M. Nistor, N. Gofar, A. Satyanaga, X. Qin, C. Y. Ip. Georisk: Assessment and Management of Risk for Engineered Systems and Geohazards. (Published online in 2020).
24. J. Herza, M. Ashley, J. Thorp. Factor of Safety-Do we use it correctly? ANCOLD Conference. https://www.researchgate.net/profile/James-Thorp-6/publication/327920961_Factor_of_Safety-Do_we_use_it_correctly/links/5bad713492851ca9ed2b8025/Factor-of-Safety-Do-we-use-it-correctly.pdf; (2017).
25. M. K., Malik, I. Karim. Materials Science and Engineering, January, Vol. **928**. Doi:10.1088/1757-899X/928/2/022074; (2020).
26. Y. Chua, H. Rahardjo, A. Satyanaga. Transportation Geotechnics. 33:100727. (2022)